International Journal of Enhanced Research in Science, Technology & Engineering
ISSN: 2319-7463, Vol. 15 Issue 1, January-2026

Analysis of Performance in Wireless Powered Communication Networks Operating over Rician Fading Channels

Mamta Rani

Kalinga University, Naya Raipur, Chhattisgarh, India

ABSTRACT

This work focuses on the power beamforming of wireless powered communication networks for line-of-sight (LOS) environments. Rician fading is used in the wireless link domain (with multiple-antenna APs and single-antenna users), for which the SNR is defined as the product of two independent non-central Chi-square random variables. Following this model, we formulate specific analytic expressions for critical performance metrics (OP, EC, throughput under delay-limited and delay-tolerant scenarios, bit error rate (BER) across common modulation strategies. We also offer streamlined approximations and asymptotic statements to build upon the system's performance in operational phases. Additionally, we investigate the best optimization of the energy harvesting time with a closed form that reaches the maximum uplink throughput. The empirical observations were verified using Monte Carlo analysis, to show a perfect agreement with theoretical prediction. The work demonstrates that channel conditions, energy harvesting efficiency, and antenna settings influence the system performance overall and presents interesting research ideas for the advancement of the 6G-IoT wireless powered network.

Keywords: Line-of-sight, Beamforming, Energy, Outage, Capacity, Modulation, Harvesting.

INTRODUCTION

Energy harvesting has emerged as an effective method to extend the operational lifetime of wireless devices and, in some cases, to achieve fully battery-free operation as well. Energy can be extracted from sunlight, wind, ambient signals, and other sources, but the intermittent nature of these components often makes it impossible to guarantee a reliable level of service quality. This has spurred interest in wireless power transfer (WPT) via dedicated power transmitters as an alternative solution to support continuous power delivery[1], [2], [3]. As a result, in the field of energy harvesting (EH), detailed theoretical examination of the coupling of EH links over fading channels is critical for performance evaluation and system design.

However, the majority of existing works involve Rayleigh or Nakagami-m fading models, which assume rich scattering environments without a dominant line-of-sight (LOS) component. In actuality, many short-range microwaves power transfer scenarios (typically over 3–15 m for mobile devices, sensors, and low-power terminals[4]) exhibit a strong LOS path. In such cases, the Rician fading model provides a more accurate description of the wireless channel. Nevertheless, EH systems under Rician fading have not been extensively researched, with only limited results available in studies such as dual-hop amplify-and-forward energy harvesting relay systems[5], [6].

In practice, a hybrid access point (AP) that conveys energy in the downlink and receives data in the uplink is a common implementation of WPT. In this arrangement, a single-antenna user harvests energy from the AP and transmits information using the harvested power. This “harvest-then-transmit” principle[7] forms the basis of the well-studied wireless-powered communication network (WPCN) architecture[8], [9], widely used in wireless sensor networks, RFID systems, and emerging IoT platforms. Nonetheless, previous studies on WPCNs frequently consider non-LOS fading scenarios (e.g.,[10], [11]), which, as mentioned earlier, do not reflect realistic cases where LOS components dominate.

To bridge this gap, this work evaluates WPCNs operating over LOS-dominated channels. Our work generalizes the framework of [12] to the Rician case and further extends it by providing a detailed analysis of symbol error rate (SER) performance for widely used modulation schemes. Under LOS conditions, the received signal-to-noise ratio (SNR) at the AP is expressed as the product of two independent non-central Chi-square random variables. The probability

distribution of this product is mathematically complex and can only be expressed as an infinite series [13], [14]. Based on these foundational results, we derive exact analytical expressions for outage probability (OP), ergodic capacity (EC), and bit error rate (BER). Since the resulting expressions are complicated and computationally intensive, we also provide simplified asymptotic and approximate solutions for practical engineering applications. Both delay-limited and delay-tolerant transmission modes are examined.

The key contributions of this paper are summarized as follows:

1. Concise derivations of OP and EC for comprehensive performance evaluation under both delay-limited and delay-tolerant modes.
2. Closed-form BER expressions for binary phase-shift keying (BPSK) and binary differential phase-shift keying (BDPSK).
3. Identification of the optimal energy harvesting time for high-SNR delay-tolerant transmission.
4. Insightful asymptotic and approximate evaluations for EC, BPSK, and BDPSK to better understand system characteristics.

To our knowledge, this work is the first to present both exact and asymptotic performance analysis for the considered WPCN configuration under LOS-dominant Rician channels.

Notation: For a random variable X, $f_X(\cdot)$ and $F_X(\cdot)$ denote its probability density and cumulative distribution functions, respectively. A circularly symmetric complex Gaussian random variable with mean μ and variance σ^2 is denoted by $CN(\mu,\sigma^2)$. The gamma function $\Gamma(\cdot)$ is defined in [15], Eq. (8), and $K_v(\cdot)$ represents the modified Bessel function of the second kind. The Meijer-G function follows the definition in [15], Eq. (9). A non-central Chi-square random variable with n degrees of freedom and non-centrality parameter δ is denoted as $\chi_n^2(\delta)$, with the central case corresponding to $\delta = 0$.

METHODOLOGY

Consider a wireless powered communication network (WPCN) with multiple antennas that facilitates downlink energy transfer and uplink data communication (refer to Fig. 1). In this setup, both the hybrid access point (AP) and the single-antenna user operate in half-duplex mode. The AP is equipped with $n \geq 1$ antennas, utilizing maximum ratio combining (MRC) for receiving uplink signals while employing maximal ratio transmission (MRT) for energy beamforming during downlink operations. Following references[11], [16], we assume that the AP has access to perfect channel state information (CSI).

Let the channel for downlink energy transfer be represented as

$$h = \begin{bmatrix} h_1 \\ \vdots \\ h_k \\ \vdots \\ h_n \end{bmatrix} \in C^{n\times 1},$$

and the channel for uplink data transfer as

$$g = \begin{bmatrix} g_1 \\ \vdots \\ g_k \\ \vdots \\ g_n \end{bmatrix} \in C^{n\times 1}.$$

Each coefficient h_k and g_k ($k = 1, \ldots, n$) is modeled as an independent and identically distributed (i.i.d.) circularly symmetric complex Gaussian random variable:

$$h_k \sim \mathrm{CN}(\mu_{k,1}, \sigma_1^2), g_k \sim \mathrm{CN}(\mu_{k,2}, \sigma_2^2).$$

Consequently, the channel gains are characterized as

$$\| h \|^2 = \frac{1}{2}\sigma_1^2 X_1, \| g \|^2 = \frac{1}{2}\sigma_2^2 X_2,$$

where $X_i \sim \chi_{2n}^2(\lambda_i)$ denotes a non-central Chi-square random variable with non-centrality parameter

$$\lambda_i = \frac{2}{\sigma_i^2} \sum_{k=1}^{n} / \mu_{k,i} /^2.$$

The probability density function (PDF) of $X_i, i = 1,2,$ follows the standard non-central Chi-square distribution [17], Eq. (1).

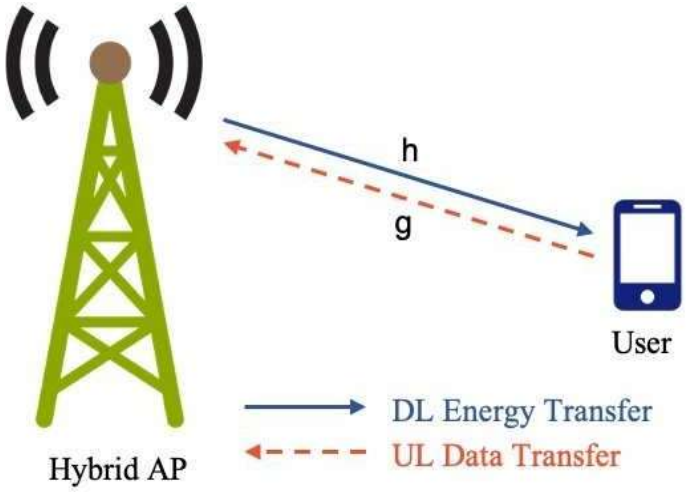

Figure 1. System Architecture

For a transmission block lasting T (with $T = 1$), the user harvests energy over a fraction τT, where $\tau \in [0,1]$, and transmits information during the remaining period $(1-\tau)T$. Therefore, the harvested energy can be expressed as
$E_h = \eta \tau P /\!/ h /\!/^2,$

where P represents the transmit power of the AP and η is the energy conversion efficiency. During the uplink phase, the signal received at the AP is given by

$$y_A = \sqrt{\frac{E_h}{1-\tau}}\, g s + n,$$

where s is the unit-energy transmit symbol and n is additive white Gaussian noise (AWGN). The resulting signal-to-noise ratio (SNR) at the AP becomes

$$\gamma_A = \frac{\tau \eta P \sigma_1^2 \sigma_2^2}{4(1-\tau) N_0} X_1 X_2 = \frac{\tau}{1-\tau} \gamma X_1 X_2, \quad ¿\(1\)$$

Where,

$$\gamma = \frac{\eta P \sigma_1^2 \sigma_2^2}{4 N_0},$$

and N_0 denotes the noise variance.
The exact PDF of the product
$Y = X_1 X_2,$
is quite intricate but can be derived via Mellin transform techniques, as discussed in [17], Eq. (11). Using this classical result, the PDF of γ_A can be written as

$$f_{\gamma_A}(y) = \sum_{m=0}^{\infty} \sum_{j=0}^{m} \psi(m,j) \frac{(1-\tau)}{\tau\gamma} \left(\frac{y(1-\tau)}{\tau\gamma} \right)^{\alpha(m)} K_{2j-m}\left(2\sqrt{\frac{y(1-\tau)}{\tau\gamma}} \right), \quad ¿\(2\)$$

Where,

- $K_n(\cdot)$ is the modified Bessel function of the second kind,
- $\alpha(m) = n + \frac{m}{2} - 1,$

$$\psi(m,j) = \frac{\lambda_1^j \lambda_2^{m-j}}{2^{1-2n-2m} j!(m-j)! \Gamma(n+j) \Gamma(n+m-j)}.$$

The special case $\lambda_1 = \lambda_2 = 0$ reduces to the Rayleigh fading scenario discussed in.

Patnaik Approximation

The PDF of the product of two non-central Chi-square random variables in (2) is difficult to evaluate due to its infinite-series form and the presence of multiple Bessel functions. Additionally, averaging error-rate expressions over such functions introduces numerical challenges. While the exact formula yields precise results, approximate expressions are often desirable for engineering insight and computational efficiency.

Patnaik [18] proposed approximating a non-central Chi-square random variable by a scaled central Chi-square variable. Following this approach, we approximate

$$X_i \approx c_i Z_i, Z_i \sim \chi^2_{v_i}(0),$$

where the constants c_i and degrees of freedom v_i are obtained by matching the first two moments of X_i and $c_i Z_i$. These yields

$$c_i = \frac{2n+2\lambda_i}{2n+\lambda_i}, v_i = \frac{(2n+\lambda_i)^2}{2n+2\lambda_i}.$$

Using these approximations, the moment-generating function (MGF) of the product $Z_1 Z_2$ becomes a useful tool.

Proposition 1.

The moment-generation function (MGF) of the product of two independent random variables

$$Z_i \sim \chi^2_{v_i}(0), i = 1,2, (3)$$

is given by

$$M_{Z_1 Z_2}(t) = \frac{1}{2^{v_2/2}} t^{-v_2/2}\, \psi\left(\frac{v_2}{2}, \frac{v_2 - v_1}{2} + 1; \frac{1}{4t}\right), \quad ¿\(4\)$$

where $\Psi(a, b; z)$ is the confluent hypergeometric function

Analytical Performance Evaluation:

A. Delay-Limited Transmission Mode

1) Exact Analysis: This transmission mode is suitable for applications that are delay-sensitive because the received signal at the AP must be decoded independently for each block. The average throughput in this case can be determined by evaluating the outage probability (OP) for a fixed transmission rate R. OP is defined as the probability that the instantaneous achievable throughput, $\log_2(1+\gamma_A)$, falls below a predetermined threshold γ_{th}.

Thus, the average throughput is expressed as

$$P_{ave} = (1 - P_{out}) R(1-\tau) = \left(1 - F_{\gamma_A}(2^{\gamma_{th}} - 1)\right) R(1-\tau), \quad ¿\(5\)$$

where $F_{\gamma_A}(y)$ is the cumulative distribution function (CDF) of γ_A. The CDF can be derived as

$$F_{\gamma_A}(y) = (a) \sum_{m=0}^{\infty} \sum_{j=0}^{m} \psi(m,j) \frac{(1-\tau)}{e^{\frac{1}{2}(\lambda_1+\lambda_2)} \tau\gamma} \int_0^y \left[\left(\frac{t(1-\tau)}{\tau\gamma} \right)^{\alpha(m)} K_{2j-m}\left(2\sqrt{\frac{t(1-\tau)}{\tau\gamma}} \right) \right] dt$$

$$¿(b) \sum_{m=0}^{\infty} \sum_{j=0}^{m} \psi(m,j) G^{2,1}_{1,3}\left(\frac{y(1-\tau)}{4\tau\gamma} \middle| \begin{matrix} \frac{2j-m}{2}, -\frac{2j-m}{2}, -\alpha(m)-1 \\ 1-\alpha(m) \end{matrix} \right) \frac{2e^{\frac{1}{2}(\lambda_1+\lambda_2)}}{\left(\frac{1-\tau}{\tau\gamma}\right)^{\alpha(m)+1}} y^{-(\alpha(m)+1)}, \quad ¿\(6\)$$

where $y = 2^{\gamma_{th}} - 1$. Step (a) follows from the definition of the CDF, while step (b) applies the integral identity from [15], Eq. (6) involving Meijer G-functions.

B. Delay-Tolerant Mode of Transmission

1) Improved Throughput Analysis:

In this transmission mode, the AP has sufficient buffering capability and can tolerate decoding delay by storing the received data. Therefore, the ergodic capacity (EC) serves as an appropriate performance metric. Since the SU uses a fraction τ of the transmission time to harvest energy, the effective time available for data transmission becomes $(1-\tau)$. Hence, the throughput is given by:

$$C = (1-\tau) \int_0^{\infty} \log_2(1+y)\, f_{\gamma_A}(y)\, dy.$$

Using the expression for $f_{\gamma_A}(y)$, this can be rewritten as:

$$¿(a)\sum_{m=0}^{\infty}\sum_{j=0}^{m}(1-\tau)2^{2\alpha(m)-1}\psi(m,j)\frac{e^{\frac{1}{2}(\lambda_1+\lambda_2)}(\tau-\tau\gamma)}{-\alpha(m)-1}\int_0^{\infty}G_{2,2}^{1,2}(y\vee 1,1;1,0)G_{0,2}^{2,0}\left(\frac{y(1-\tau)}{4\tau\gamma}\vee -\frac{\alpha(m)}{2},\frac{2j-m}{2}+\alpha(m)\right)dy.(7)$$

This leads to the expression:

$$¿(b)\sum_{m=0}^{\infty}\sum_{j=0}^{m}(1-\tau)2^{2\alpha(m)-1}\psi(m,j)\ln(2)\,e^{\frac{1}{2}(\lambda_1+\lambda_2)}(\tau-\tau\gamma)^{-\alpha(m)-1}G_{2,4}^{4,1}\left(\frac{1}{4\tau\gamma}\vee -1,0;-1,-1,\frac{2j-m}{2}+\alpha(m),-\frac{2j-m}{2}+\alpha(m)\right).$$

To obtain this expression from Eq. (7), we express $\ln(1+x)$ and $K_n(x)$ in terms of Meijer G-functions following, Eq. (12), and then substitute these identities back into the original equation for C. This results in the asymptotic solution presented in the next proposition.

2) Asymptotic Throughput Analysis

Proposition 2. The asymptotic capacity of the delay-tolerant transmission mode is given by

$$C=\frac{1-\tau}{\ln 2}\left[\ln(\acute{\gamma})+D-\ln\left(\frac{1-\tau}{\tau}\right)\right],\quad ¿\(8\)$$

as $\acute{\gamma}\to\infty$, where,

$$D=\ln(c_1)+\ln(c_2)+\psi\left(\frac{v_1}{2}\right)+\psi\left(\frac{v_2}{2}\right)+2\ln(2),$$

and $\psi(\cdot)$ is the Euler psi function, Eq. (8).
Also,

$$\acute{\gamma}=\frac{\eta P\sigma_1^2\sigma_2^2}{4N_0}.$$

Proof. Let

$$C=(1-\tau)C^{¿},$$

Where,

$$C^{¿}=E[\log_2(1+\gamma_A)].$$

For large $\acute{\gamma}$, we obtain

$$C^{¿}\approx\left[\log_2\left(\frac{\tau}{1-\tau}\acute{\gamma}\right)+E[\log_2(X_1)]+E[\log_2(X_2)]\right],\quad ¿\(9\)$$

which may further be expressed as

$$C^{¿}\approx\left[\log_2\left(\frac{\tau}{1-\tau}\acute{\gamma}\right)+E[\log_2(c_1Z_1)]+E[\log_2(c_2Z_2)]\right].$$

When $\acute{\gamma}\to\infty$, we use

$$E[\log(Z)]=\frac{dE[Z^{t-1}]}{dt}\Big/_{t=1}.$$

If $Z\sim\chi_v^2(0)$, then

$$E[Z^{t-1}]=2^{t-1}\frac{\Gamma(t+v/2-1)}{\Gamma(v/2)}.$$

The asymptotic capacity expression in (8) can then be used to obtain a closed-form approximation for the optimal energy-harvesting time fraction $\tau^{¿}$ at high SNR. The derivation, similar to Appendix B in [19], is omitted. The resulting approximation is

$$\tau^{¿}\approx\frac{1}{1+W(\acute{\gamma}e^{D-1})},\quad ¿\(10\)$$

where the Lambert W function satisfies $W(x)e^{W(x)}=x$, and $W(x)$ is monotonic for $x\geq 0$.

C. Average Bit Error Rate

The average bit error rate (BER) of the system can be computed by averaging the conditional error probability $P_e(y)$ over the PDF of γ_A, denoted by $f_{\gamma_A}(y)$. These yields

$$\acute{P}_{BER}=\int_0^{\infty} P_e(y)\, f_{\gamma_A}(y)\, dy.$$

1) Exact BER of BPSK: Binary phase-shift keying (BPSK) is widely used due to its simplicity and robustness in noisy environments. According to Eq. (8), the conditional BER of BPSK can be substituted directly into the above expression. Using that relation, the average BER becomes

$$\acute{P}_{BER}=\sum_{m=0}^{\infty}\sum_{j=0}^{m} a\,\psi(m,j)\frac{(1-\tau)}{b e^{\frac{1}{2}(\lambda_1+\lambda_2)}\tau\gamma\sqrt{\pi}}2^{\alpha(m)-1}G_{2,3}^{2,3}\left(\frac{1-\tau}{4b\tau\gamma}\middle|\begin{matrix}0,-\frac{1}{2}\\ \frac{2j-m}{2}+\alpha(m),-\frac{2j-m}{2}+\alpha(m),-1\end{matrix}\right), \quad ¿\(11\)$$

Where,

$$a=\frac{1}{2}, b=1.$$

2) Approximate BER of BPSK

An alternate approximation uses the well-known representation

$$\acute{P}_{BER,app}=E_{\gamma}\left[a\,erfc\left(\sqrt{b\gamma_A}\right)\right].$$

Step-by-step, this becomes

$$¿(a)\,E\left[\frac{a}{\pi}\int_{-\frac{\pi}{2}}^{\frac{\pi}{2}}\exp\left(\frac{-b\gamma_A}{\sin^2\theta}\right)d\theta\right] ¿(b)\,\frac{a}{\pi}\int_{-1}^{1}E_{\gamma}\left[\exp\left(\frac{-b\gamma_A}{1-t^2}\right)\right]\frac{dt}{\sqrt{1-t^2}} ¿(c)\,\frac{a}{\pi}\int_{-1}^{1}M_{Z_1Z_2}\left(\frac{u}{1-t^2}\right)\frac{dt}{\sqrt{1-t^2}}$$

$$¿(d)\,\frac{a}{w}\sum_{k=1}^{w}M_{Z_1Z_2}\left(\frac{u}{t_k^2}\right), \quad ¿\(12\)$$

where:

- (a) uses the standard erfc integral representation,
- (b) substitutes $\sin\theta=t$,
- (c) applies Proposition 1 with $u=\frac{\tau}{1-\tau}\gamma c_1 c_2$,
- (d) follows from Gauss-Chebyshev quadrature, where $t_k=\cos\left(\frac{(2k-1)\pi}{2w}\right)$ and w is the number of quadrature nodes.

3) Exact BER of BDPSK

For binary differential phase-shift keying (BDPSK), the conditional BER is given by Using the MGF-based formulation in and the MGF of γ_A from, Eq. (4), the average BER becomes

$$P_e(y)=ae^{-by}.$$

$$\acute{P}_{BER}=\sum_{m=0}^{\infty}\sum_{j=0}^{m} a\,\psi(m,j)\frac{\left(1-\tau\right)^{\alpha(m)+\frac{1}{2}}}{2e^{\frac{1}{2}(\lambda_1+\lambda_2)}(\tau\gamma)^{\alpha(m)+\frac{1}{2}}}\Delta\, e^{\frac{1}{4\tau\gamma}}W_{-\alpha(m)-\frac{1}{2},\frac{2j-m}{2}}\left(\frac{1-\tau}{4\tau\gamma}\right), \quad ¿\(13\)$$

Where,

$$\Delta = \frac{\Gamma,\left(\alpha(m)+j-\frac{m}{2}+1\right)}{\Gamma,\left(\alpha(m)-j+\frac{m}{2}+1\right)},$$

and $W_{\lambda,\mu}(\cdot)$ is the Whittaker function [9, Eq. (9)]. For BDPSK,

$$a=\frac{1}{2}, b=1.$$

4) Approximate BER of BDPSK

Although the exact BER in (13) is precise, it requires evaluating an infinite series, which may be computationally demanding. A more convenient approximation can be derived using the Patnaik approximation (Section II-A). Applying it gives

$$\acute{P}_{BER,app}=E\left[ae^{-b\frac{\tau}{1-\tau}\gamma X_1 X_2}\right]=E\left[ae^{-uZ_1Z_2}\right],$$

where

$$u=b\frac{\tau}{1-\tau}\gamma c_1 c_2.$$

Thus, using Proposition 1,

$$\acute{P}_{BER,app}=\frac{a}{2^{v_2/2}u^{v_2/2}}\Psi,\left(\frac{v_2}{2},\frac{v_2-v_1}{2}+1;\frac{1}{4u}\right), \quad ¿\backslash(14\backslash)$$

where $\Psi(a,b;z)$ is the confluent hypergeometric function.

Numerical Analysis and Simulation Outcomes:

The analytical formulas are validated using Monte Carlo simulations. The duration of the transmission block is set to $T=1$, and the noise variances are chosen as $\sigma_1^2=\sigma_2^2=1$. The exact results, expressed in infinite series, are computed as follows: let

$$W_m=\sum_{i=1}^{m}Q_i, W_0=0, W_m=W_{m-1}+Q_m.$$

The evaluation of the series concludes when

$$\frac{Q_m}{W_m}\leq 0.01.$$

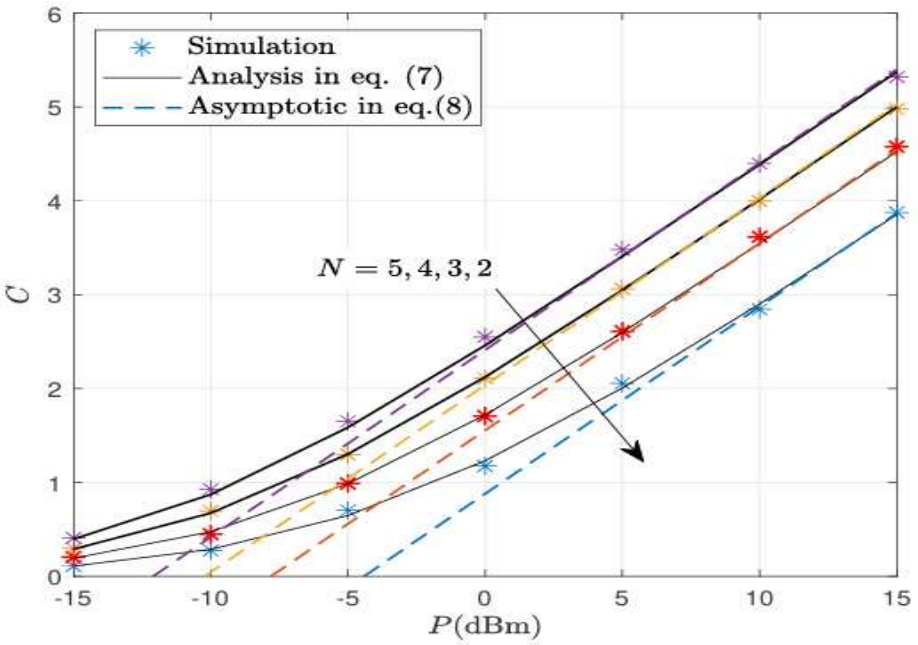

Figure 2. Average throughput of the delay-limited mode versus the Rician K-factor for $\tau = 0.4$, $\lambda_1 = \lambda_2 = K$, $N = 4$, and $\gamma_{th} = 1$ dBm.

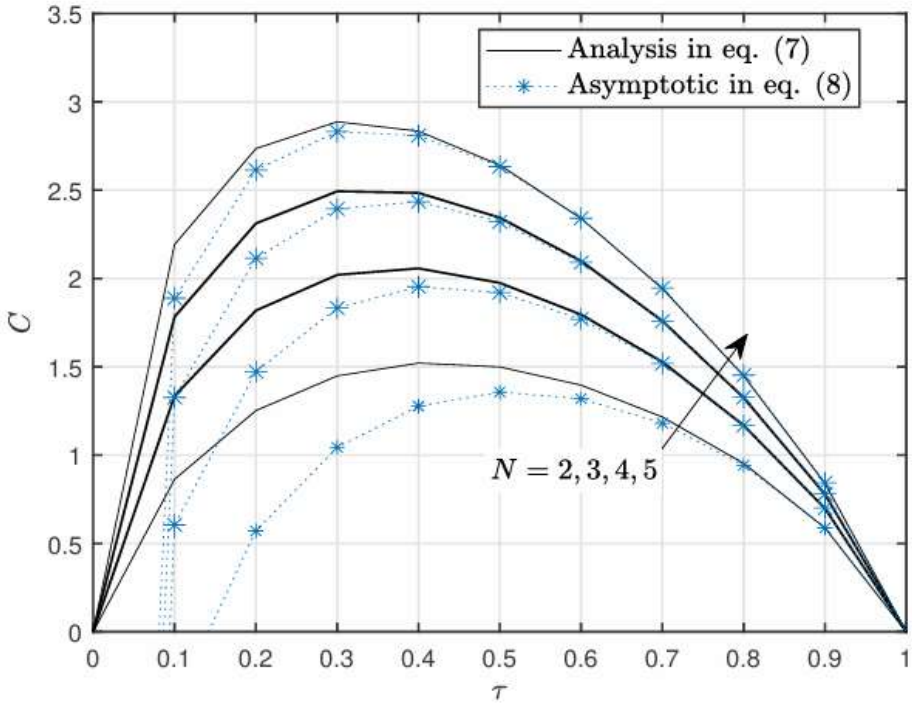

Figure 3.Average throughput of the delay-tolerant mode as a function of P for η = 0.9, τ = 0.4, and λ₁ = λ₂ = 2.

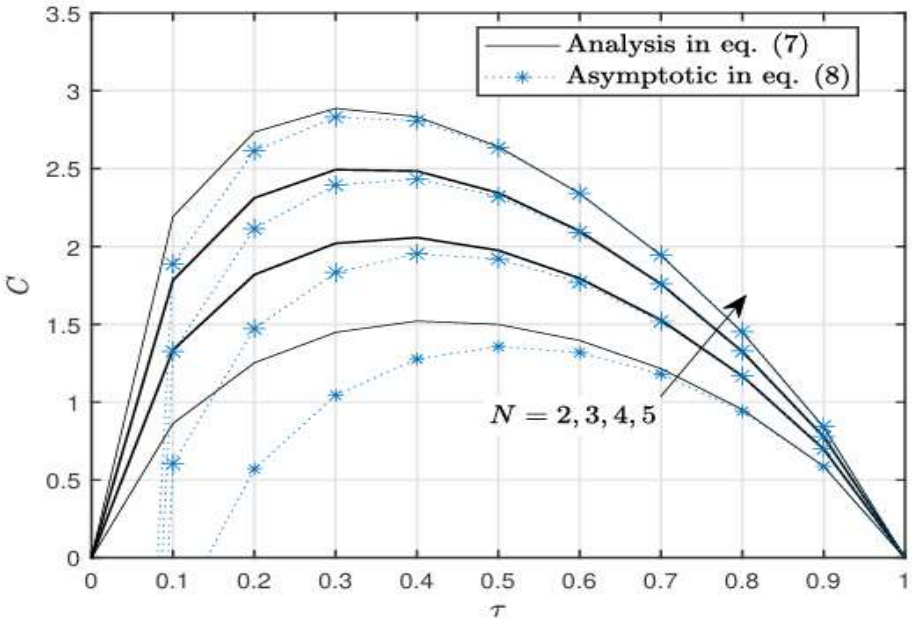

Figure 4. Average throughput of the delay-tolerant mode versus τ for $\eta = 0.9$, $P = 1$ dBm, and $\lambda_1 = \lambda_2 = 1.5$.

Fig. 2 shows the delay-limited average throughput of the LOS network as a function of the Rician K-factor for varied transmit power at the AP and changing energy conversion efficiencies at the user. The analytical curves strongly confirm the simulation results obtained and indicate the correctness of (5). The Rician K-factor of the power on the direct LOS path and multipath scattered components is described. A value of $K = 0$ denotes Rayleigh fading and $K \to \infty$ is the non-fading channel. The delay-limited throughput increases with the Rician K-factor. The better it is the greater the energy conversion efficiency, and the higher the transmit power, as a higher proportion of energy will be captured in downlink, leading to more available transmit power in uplink. Fig. 3 is the delay-tolerant throughput versus AP transmit power. Although the asymptotic curves in (8) deviate from the exact expressions in (7) at low transmit power levels, they converge very rapidly with increasing power. Throughput increases with both the increase in transmit power and the number of antennas at the AP. Moreover, with the simulation curves closely mirroring the analytical result, the precision of the derived expressions is demonstrated.

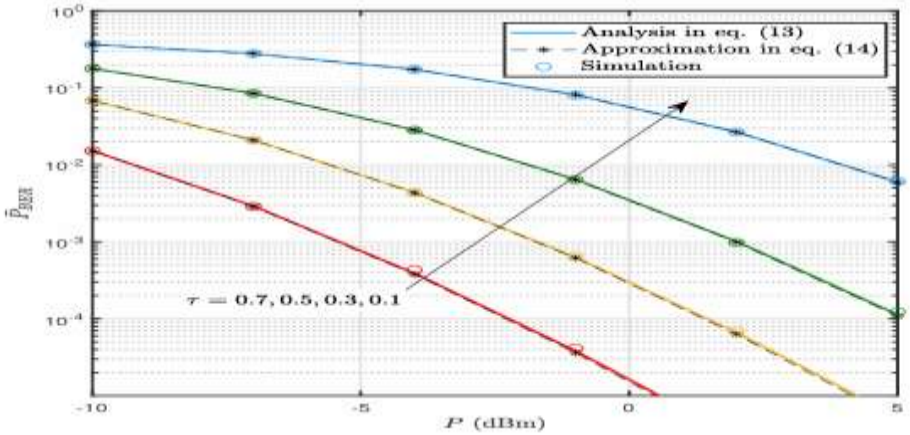

Figure 5. Bit error rate (BER) of BDPSK as a function of P for n = 5, η = 0.9, and λ₁ = λ₂ = 2.

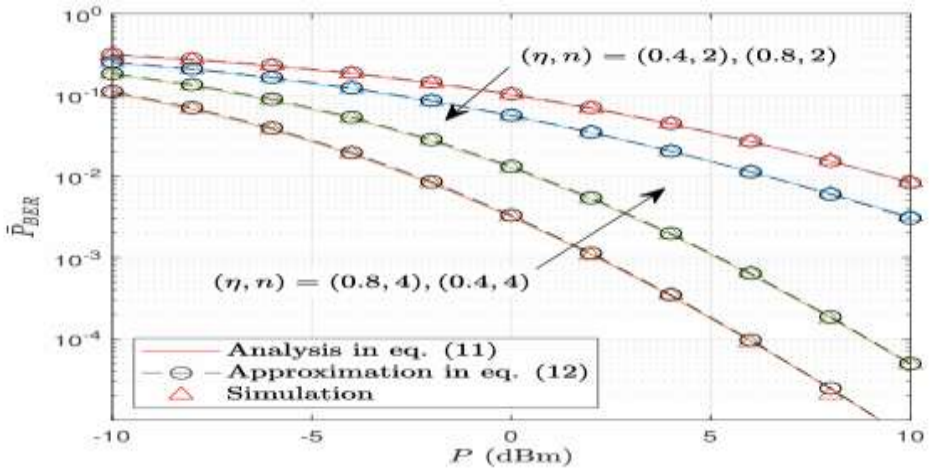

Figure 6. Bit error rate (BER) of BPSK as a function of P for n = 5, τ = 0.4, and λ₁ = λ₂ = 1.

Fig. 4 shows the throughput versus the energy harvesting duration τ in the delay-tolerant mode for different numbers of AP antennas. The number of antennas determines the optimal value of τ, consistent with the analytical expression in (10). Since the user harvests energy during a fraction τ of the block and transmits during the remaining $(1-\tau)$, the optimal harvesting time $\tau^{¿}$ represents a balance between these two operations. Furthermore, as both the energy harvesting duration and the number of AP antennas increase, the asymptotic curves in equation (8) approach the exact results given in equation (7).

Figs. 5 and 6 present the bit error rate (BER) performance for Binary Differential Phase Shift Keying (BDPSK) and Binary Phase Shift Keying (BPSK), respectively, as a function of the AP transmit power. The close agreement among the exact analytical results, simulations, and approximations confirms the accuracy of equations (11) and (13), as well as the validity of the Patnaik approximation (Proposition 1). In both cases, the BER improves as the AP transmit power increases, because higher transmit power yields a higher signal-to-noise ratio (SNR) at the receiver, thereby enhancing link reliability. Moreover, longer energy harvesting durations lead to reduced BER since the user has a larger power budget for uplink transmission.

Additionally, Fig. 6 demonstrates that the BER of BPSK decreases as either the number of AP antennas or the energy harvesting efficiency increases, highlighting the benefits of greater system diversity and improved energy conversion efficiency.

CONCLUSION

A comprehensive performance analysis of energy beamforming in a WPCN operating over LOS channels has been presented. This work fills a gap in the literature by examining a system configuration composed of a multiple-antenna AP and a single-antenna, batteryless user device. The user harvests energy from the AP's downlink transmissions and subsequently sends data in the uplink. Exact and approximate/asymptotic expressions for OP, EC, and BER were derived and validated using Monte Carlo simulations.

The key findings of this study can be summarized as follows:

1. The outage probability (OP), ergodic capacity (EC), and bit error rate (BER) all improve with increased AP transmit power and with a larger number of AP antennas.
2. System performance enhances as the Rician K-factor increases in strong LOS conditions. Interestingly, the optimal energy harvesting time fraction remains largely unaffected by variations in the K-factor.

REFERENCES

[1]. S. Sudevalayam and P. Kulkarni, "Energy Harvesting Sensor Nodes: Survey and Implications," *IEEE Communications Surveys & Tutorials*, vol. 13, no. 3, pp. 443–461, 2011, doi: 10.1109/SURV.2011.060710.00094.

[2]. J. A. Paradiso and T. Starner, "Energy Scavenging for Mobile and Wireless Electronics," *IEEE Pervasive Comput*, vol. 4, no. 1, pp. 18–27, Jan. 2005, doi: 10.1109/MPRV.2005.9.

[3]. R. Zhang and C. K. Ho, "MIMO Broadcasting for Simultaneous Wireless Information and Power Transfer," *IEEE Trans Wirel Commun*, vol. 12, no. 5, pp. 1989–2001, May 2013, doi: 10.1109/TWC.2013.031813.120224.

[4]. M. K. Simon and M. Alouini, *Digital Communication over Fading Channels*. Wiley, 2004. doi: 10.1002/0471715220.
[5]. J. Chown, W. Scharfman, and T. Morita, "Voltage Breakdown Characteristics of Microwave Antennas," *Proceedings of the IRE*, vol. 47, no. 8, pp. 1331–1337, Aug. 1959, doi: 10.1109/JRPROC.1959.287199.
[6]. H. Hashemi, "The indoor radio propagation channel," *Proceedings of the IEEE*, vol. 81, no. 7, pp. 943–968, Jul. 1993, doi: 10.1109/5.231342.
[7]. Z. Chu, P. Xiao, D. Mi, H. Chen, and W. Hao, "Intelligent reflecting surfaces enabled cognitive internet of things based on practical pathloss model," *China Communications*, vol. 17, no. 12, pp. 1–16, Dec. 2020, doi: 10.23919/JCC.2020.12.001.
[8]. L. Velasco *et al.*, "A service-oriented hybrid access network and clouds architecture," *IEEE Communications Magazine*, vol. 53, no. 4, pp. 159–165, Apr. 2015, doi: 10.1109/MCOM.2015.7081090.
[9]. Z. Chu, P. Xiao, D. Mi, H. Chen, and W. Hao, "Intelligent reflecting surfaces enabled cognitive internet of things based on practical pathloss model," *China Communications*, vol. 17, no. 12, pp. 1–16, Dec. 2020, doi: 10.23919/JCC.2020.12.001.
[10]. L. Velasco *et al.*, "A service-oriented hybrid access network and clouds architecture," *IEEE Communications Magazine*, vol. 53, no. 4, pp. 159–165, Apr. 2015, doi: 10.1109/MCOM.2015.7081090.
[11]. Z. Chu, P. Xiao, D. Mi, H. Chen, and W. Hao, "Intelligent reflecting surfaces enabled cognitive internet of things based on practical pathloss model," *China Communications*, vol. 17, no. 12, pp. 1–16, Dec. 2020, doi: 10.23919/JCC.2020.12.001.
[12]. Z. Chu, P. Xiao, D. Mi, H. Chen, and W. Hao, "Intelligent reflecting surfaces enabled cognitive internet of things based on practical pathloss model," *China Communications*, vol. 17, no. 12, pp. 1–16, Dec. 2020, doi: 10.23919/JCC.2020.12.001.
[13]. M.-S. Alouini and M. K. Simon, "An MGF-based performance analysis of generalized selection combining over Rayleigh fading channels," *IEEE Transactions on Communications*, vol. 48, no. 3, pp. 401–415, Mar. 2000, doi: 10.1109/26.837044.
[14]. S. Liu, "On local influence for elliptical linear models," *Statistical Papers*, vol. 41, no. 2, pp. 211–224, Apr. 2000, doi: 10.1007/BF02926104.
[15]. I. S. ; R. I. M. Gradshteyn, *Table of Integrals, Series, and Products*, 7th ed. Amsterdam, The Netherlands: Academic Press, 2007.
[16]. A. Akbarpour-Kasgari and M. Ardebilipour, "Pilot allocation approaches for channel estimation in MIMO relay networks," *IET Communications*, vol. 12, no. 16, pp. 2030–2037, Oct. 2018, doi: 10.1049/iet-com.2017.0994.
[17]. M.-S. Alouini and M. K. Simon, "An MGF-based performance analysis of generalized selection combining over Rayleigh fading channels," *IEEE Transactions on Communications*, vol. 48, no. 3, pp. 401–415, Mar. 2000, doi: 10.1109/26.837044.
[18]. P. B. PATNAIK, "THE NON-CENTRAL χ 2 - AND *F* -DISTRIBUTIONS AND THEIR APPLICATIONS," *Biometrika*, vol. 36, no. 1–2, pp. 202–232, 1949, doi: 10.1093/biomet/36.1-2.202.
[19]. Q. Liu, "Human motion state recognition based on MEMS sensors and Zigbee network," *Comput Commun*, vol. 181, pp. 164–172, Jan. 2022, doi: 10.1016/j.comcom.2021.10.018.